Mathematical Biosciences and Engineering

http://www.aimspress.com/journal/mbe

MBE, 20(7): 12599–12624.
DOI: 10.3934/mbe.2023561
Received: 17 February 2023
Revised: 12 April 2023
Accepted: 09 May 2023
Published: 26 May 2023

Research article

Dynamics of a harvested cyanobacteria-fish model with modified Holling type IV functional response

Shengyu Huang[1,2], Hengguo Yu[1,2], Chuanjun Dai[1,3], Zengling Ma[1,3], Qi Wang[1,3] and Min Zhao[1,3,*]

[1] Key Laboratory for Subtropical Oceans & Lakes Environment and Biological Resource Utilization Technology of Zhejiang, Wenzhou University, Wenzhou 325035, China

[2] School of Mathematics and Physics, Wenzhou University, Wenzhou 325035, China

[3] School of Life and Environmental Science, Wenzhou University, Wenzhou 325035, China

* **Correspondence:** Email: zmcn@tom.com.

Abstract: In this paper, considering the aggregation effect and Allee effect of cyanobacteria populations and the harvesting of both cyanobacteria and fish by human beings, a new cyanobacteria-fish model with two harvesting terms and a modified Holling type IV functional response function is proposed. The main purpose of this paper is to further elucidate the influence of harvesting terms on the dynamic behavior of a cyanobacteria-fish model. Critical conditions for the existence and stability of several interior equilibria are given. The economic equilibria and the maximum sustainable total yield problem are also studied. The model exhibits several bifurcations, such as transcritical bifurcation, saddle-node bifurcation, Hopf bifurcation and Bogdanov-Takens bifurcation. It is concluded from a biological perspective that the survival mode of cyanobacteria and fish can be determined by the harvesting terms. Finally, concrete examples of our model are given through numerical simulations to verify and enrich the theoretical results.

Keywords: cyanobacteria-fish model; Allee effect; harvesting; aggregation effect; bifurcation

1. Introduction

Cyanobacteria are the oldest photosynthesizers and they have promoted the formation of the biosphere on the earth. However, cyanobacteria are increasingly becoming dominant among other phytoplankton with the concentrations of TP and TN increasing in the eutrophication process of rivers and lakes. Compared with other beneficial phytoplankton, cyanobacteria bloom will produce various toxic secondary metabolites (for example, cyanotoxins) [1,2], which will further cause certain damage to the natural ecosystems and human health. Nevertheless, cyanobacteria can be regarded as a potential solar

biorefinery and continuously provide biofuels and chemicals when used properly [3–5]. Harvesting cyanobacteria can greatly reduce TP, TN and other nutrients and then effectively prevent the deterioration of water eutrophication. The harvested cyanobacteria can be processed into compound organic fertilizer, organic biogas fertilizer as well as biogas with energy value for power generation or deep comprehensive utilization. Thus, artificial harvesting of cyanobacteria can serve a dual purpose in aquatic environments where cyanobacteria blooms occur. Among the various methods to control cyanobacteria bloom, the biological method based on the predation relationship between fish and cyanobacteria populations is widely used for its effectiveness, harmlessness and economic benefits. In recent years, researchers have done a lot of research on the control of algae by fish and zooplankton [6, 7]. And mathematical researchers usually use differential equation models to analyze the dynamic relationship between species; the predator-prey model has been widely studied by researchers [8–11] since it was put forward. On the other hand, the extensive human demand for fish resources has also prompted the cultivation and harvesting of fish in as many water ecosystems as possible. Considering the growth rates, biomasses and harvesting intensities of cyanobacteria and fish, a reasonable harvesting plan should be made by the managers of biological resources to maintain sustainable fish resources and a low density of cyanobacteria population.

The harvesting term is a vital element in ecological models, since it has great significance for the development of species population and economic growth. A previous paper [12] explored the harvesting of biological resources, utilizing a delayed reaction diffusion three-species model, and presented the conclusion that the harvesting terms significantly affect the existence of species. Another group [13] found that there exists a bistable region of their model when a Michaelis-Menten harvesting term for the predator population was introduced; they also derived the threshold of harvesting efforts to achieve the maximum economic benefits under the premise of sustainable development. The authors of [14] proposed a deterministic and stochastic fractional-order model of a tri-trophic food chain with a harvesting term, and they concluded that the dynamics of the second predator can be controlled by the harvesting parameters. The authors of [15] concluded that the harvesting term plays an important role in the dynamic properties of a predator-prey model with a nonlinear harvesting term and a square root type functional response for prey. More influence of harvesting on dynamic behaviors has been investigated in [16–19].

The Allee effect is a research hotspot in the field of population dynamics. The study of it helps to understand the survival and reproductive mechanisms of species. It is also of great significance for the conservation of endangered species. The authors of [20] investigated a predator-prey diffusion model with a strong Allee effect, and the results showed that a small initial value of prey population would lead to the extinction of both populations. The model studied in [21] can undergo a saddle-node bifurcation when the intensity of the Allee effect at the tipping point without delay and diffusions. The Allee effect has also received extensive attention in infectious disease models, and the authors of [22] demonstrated that both strong and weak Allee effects have a significant impact on the spread of infectious diseases. Further studies on the Allee effect can be found in [23–25].

Furthermore, there are many papers that have introduced a prey refuge term to the interaction mathematical model [26–28]. The authors of [29] proposed a modified algae-fish model:

$$\begin{cases} \dfrac{dx}{dt} = r_1 x\left(1-\dfrac{x}{k}\right)\left(\dfrac{x}{n}-1\right) - y\dfrac{\alpha_1 (x-m)}{a+x-m}, \\ \dfrac{dy}{dt} = \beta_1 y\dfrac{\alpha_1 (x-m)}{a+x-m} + r_2 y\left(1-\dfrac{x-m}{k}\right) - dy; \end{cases} \tag{1.1}$$

they then explained the influence on the dynamic properties of it caused by prey refuge and the Allee effect. The functional response function represents the biomass of prey captured by each predator in unit time, and it is always used to express the dynamics of predator and prey. This function represents the flow of matter from the prey population to the predator population. A modified Holling type II functional response function was constructed in model (1.1) according to the prey refuge. However, the function $\frac{\alpha(x-m)y}{a+b(x-m)+(x-m)^2}$ is more practical, which is an improved Holling type IV and it can show such a phenomenon that the defense ability of cyanobacteria population is improved after aggregation. It is also worth mentioning that the harvesting terms of algae and fish by human beings are not considered in [29]. Therefore, in order to effectively control the outbreak of cyanobacteria blooms, this paper mainly considers the physical harvesting strategy to control the outbreak of cyanobacteria blooms, and it implements the cycling mechanism of biological control of algae growth. At the same time, utilizing the bifurcation dynamics evolution behavior of ecological models, we not only explore the feasibility of a physical harvesting strategy and biological control technologies, but we also discover the interaction mechanism between fish and cyanobacteria, which can provide some theoretical support and numerical simulations for the implementation of physical spraying algae control technology in Taihu South Lake. In this paper, we study the following cyanobacteria-fish model with two harvesting terms:

$$\begin{cases} \dfrac{dx}{dt} = r_1 x\left(1-\dfrac{x}{k}\right)\left(\dfrac{x}{n}-1\right) - \dfrac{\alpha (x-m) y}{a+b(x-m)+(x-m)^2} - q_1\gamma E x, \\ \dfrac{dy}{dt} = \beta\dfrac{\alpha (x-m) y}{a+b(x-m)+(x-m)^2} - d_1 y - q_2 E y, \end{cases} \tag{1.2}$$

where E is the harvesting effort of fish, γ is the proportional coefficient of harvesting effort between fish and cyanobacteria and q_i $(i = 1, 2)$ represents the catchability coefficients of cyanobacteria and fish respectively. The biological significance of other parameters in model (1.2) is consistent with that in [29]. For the convenience of discussion, we do the following parameter substitutions to reduce the number of parameters:

$$\tau = \alpha t,\ r = \frac{r_1}{\alpha},\ d = \frac{d_1}{\alpha},\ e_1 = \frac{q_1\gamma E}{\alpha},\ e_2 = \frac{q_2 E}{\alpha},$$

retanining t to denote τ then model (1.2) can be expressed as follows:

$$\begin{cases} \dfrac{dx}{dt} = rx\left(1-\dfrac{x}{k}\right)\left(\dfrac{x}{n}-1\right) - \dfrac{(x-m) y}{a+b(x-m)+(x-m)^2} - e_1 x \overset{def}{=\!=} g^1(x,y), \\ \dfrac{dy}{dt} = \beta\dfrac{(x-m) y}{a+b(x-m)+(x-m)^2} - dy - e_2 y \overset{def}{=\!=} g^2(x,y). \end{cases} \tag{1.3}$$

The rest of the present paper is organized as follows. In Section 2, we give the critical conditions for the existence and stability of each equilibrium. The economic equilibrium and the maximum sustainable total yield problem for model (1.3) are studied in Section 3. In Section 4, we discuss the local

bifurcations of model (1.3), such as transcritical bifurcation, saddle-node bifurcation, Hopf bifurcation and Bogdanov-Takens bifurcation. With the help of numerical simulation, the dynamic behaviors of model (1.3) are studied when bifurcation occurs in Section 5. Finally, the paper ends with brief concluding remarks in Section 6.

2. Analysis of equilibria

In this section, we will discuss the critical conditions for the existence and stability of potential equilibria in model (1.3).

It is obvious that the trivial equilibrium $E_0(0,0)$ of model (1.3) always exists, and there exists a predator-free equilibrium $(x_1,0)$ $[res.\ (x_2,0)]$ when $\Delta_1 \geq 0$ and $x_1 \geq m$ $[res.\ x_2 \geq m]$, where

$$x_1 = \frac{kr + nr - \sqrt{\Delta_1}}{2r},\ x_2 = \frac{kr + nr + \sqrt{\Delta_1}}{2r},\ \Delta_1 = r^2(k-n)^2 - 4re_1nk.$$

Otherwise, model (1.3) will have two interior equilibria $\left(x_1^*, y_1^*\right)$ and $\left(x_2^*, y_2^*\right)$ when $\Delta_2 \geq 0$; x_1^* and x_2^* are the zeros of the function $f(x)$, where

$$f(x) = -(d+e_2)(x-m)^2 + [\beta - (d+e_2)b](x-m) - a(d+e_2),$$

and the expression of the two interior equilibria can be written as follows:

$$x_1^* = m - \frac{b}{2} + \frac{\beta - \sqrt{\Delta_2}}{2(d+e_2)},\ \ x_2^* = m - \frac{b}{2} + \frac{\beta + \sqrt{\Delta_2}}{2(d+e_2)},$$

where

$$\Delta_2 = (bd + be_2 - \beta)^2 - 4a(d+e_2)^2;$$

correspondingly, the expression of y_i^* $(i = 1, 2)$ can be expressed as follows:

$$y_i^* = \frac{\left[a + b\left(x_i^* - m\right) + \left(x_i^* - m\right)^2\right]\left[rx_i^*\left(1 - \frac{x_i^*}{k}\right)\left(\frac{x_i^*}{n} - 1\right) - e_1x_i^*\right]}{x_i^* - m}.$$

It is worth mentioning that $y_i^* > 0$ satisfied the biological significance when $x_1 < x_1^* \leq x_2^* < x_2$.

The interior equilibrium $E_1^*\left(x_1^*, y_1^*\right)$ $\left[res.\ E_2^*\left(x_2^*, y_2^*\right)\right]$ exists under the biological significances when (1), (2) and (3) $[res.\ (4)]$ of the following conditions are satisfied:

(1) $\beta > b(d+e_2)$,

(2) $\Delta_1 > 0, \Delta_2 > 0$,

(3) $k + n + b - 2m - \frac{\sqrt{\Delta_1}}{r} < \frac{\beta - \sqrt{\Delta_2}}{d+e_2} < k + n + b - 2m + \frac{\sqrt{\Delta_1}}{r}$,

(4) $k + n + b - 2m - \frac{\sqrt{\Delta_1}}{r} < \frac{\beta + \sqrt{\Delta_2}}{d+e_2} < k + n + b - 2m + \frac{\sqrt{\Delta_1}}{r}$.

By model (1.3), the Jacobian matrix at $E(x,y)$ can be expressed as follows:

$$J_{E(x,y)} = \begin{pmatrix} a_{11}(x,y) & a_{12}(x) \\ a_{21}(x,y) & a_{22}(x) \end{pmatrix},$$

where

$$a_{11}(x,y) = -\frac{3r}{nk}x^2 + 2r\left(\frac{1}{n}+\frac{1}{k}\right)x - r + \frac{y\left(m^2-2mx+x^2-a\right)}{\left[(x-m)^2+b(x-m)+a\right]^2} - e_1,$$

$$a_{12}(x) = -\frac{x-m}{(x-m)^2+b(x-m)+a},$$

$$a_{21}(x,y) = -\frac{\beta y\left(m^2-2mx+x^2-a\right)}{\left[(x-m)^2+b(x-m)+a\right]^2},$$

$$a_{22}(x) = \frac{\beta(x-m)}{(x-m)^2+b(x-m)+a} - d - e_2.$$

Based on the above analysis, we have the following theorems about the stability of the equilibria from the viewpoint of mathematics.

Theorem 1. Trivial extinction equilibrium $E_0(0,0)$ always exists and is a stable equilibrium.

Proof. The value of m must be equal to zero when $x = 0$ since the biomass of cyanobacteria must be greater than the aggregation amount according to the definition of model (1.3) in the biological sense; therefore the Jacobian matrix of E_0 can be written as follows:

$$J_{E_0(0,0)} = \begin{pmatrix} -r-e_1 & 0 \\ 0 & -d-e_2 \end{pmatrix};$$

it is obvious that matrix $J_{E_0(0,0)}$ has two negative characteristic roots $\lambda_1 = -r - e_1$ and $\lambda_2 = -d - e_2$. Therefore E_0 is stable according to the Routh-Hurwitz criterion. □

Theorem 2. The predator-free equilibrium $E_1(x_1,0)$ is always unstable whenever it exists. E_1 is an unstable node or focus when the following three conditions are satisfied:

(1) $\Delta_1 > 0$,
(2) $\Delta_2 > 0$,
(3) $x_1 \in [m,k] \cap \left[x_1^*, x_2^*\right]$;

otherwise E_1 is a saddle under the following three conditions:

(4) $\Delta_1 > 0$,
(5) $x_1 \in [m,k]$,
(6) $\Delta_2 < 0 \vee x_1 \notin \left[x_1^*, x_2^*\right]$.

Proof. We know that x_1 is one of the roots of the equation $g^1(x,0) = 0$ according to the previous definition. It can be easily obtained that $a_{11}(x_1,0) = \left.\frac{dg^1(x,0)}{dx}\right|_{x=x_1} > 0$ for $0 < x_1 < x_2$ based on the properties of the cubics function $g^1(x,0)$. Since $a_{21}(x_1,0) = 0$, then $a_{11}(x_1,0)$ is one of the characteristic roots of the Jacobian matrix $J_{E_1(x_1,0)}$ and another root is $a_{22}(x_1,0)$. It is only when the two conditions (2) and (3) are satisfied that $a_{22}(x_1,0) > 0$, which means that both the two characteristic roots of $J_{E_1(x_1,0)}$ are positive, then, E_1 is an unstable node or focus. Otherwise, $a_{22}(x_1,0) < 0$ when the conditions (5) and (6) are satisfied, then, the equilibrium E_1 is a saddle since the two roots have opposite signs. □

Theorem 3. The other predator-free equilibrium $E_2(x_2, 0)$ is a saddle when the following three conditions are satisfied:

(1) $\Delta_1 > 0$,

(2) $\Delta_2 > 0$,

(3) $x_2 \in [m, k] \cap \left[x_1^*, x_2^*\right]$;

otherwise it is a locally asymptotically stable node or focus under the following three conditions:

(4) $\Delta_1 > 0$,

(5) $x_2 \in [m, k]$,

(6) $\Delta_2 < 0 \vee x_2 \notin \left[x_1^*, x_2^*\right]$.

Proof. Obviously, x_2 is also a root of equation $g^1(x, 0) = 0$, and we can obtain $a_{11}(x_2, 0) = \frac{dg^1(x,0)}{dx}\Big|_{x=x_2} < 0$ through a similiar analysis. The element $a_{11}(x_2, 0)$ is one of the characteristic roots of the Jacobian matrix $J_{E_2(x_2,0)}$ since $a_{21}(x_2, 0) = 0$, and the other root is $a_{22}(x_2, 0)$. The inequality $a_{22}(x_2, 0) > 0$ will hold if and only if the conditions (2) and (3) are satisfied; in which case the Jacobian matrix $J_{E_2(x_2,0)}$ has two characteristic roots with opposite signs; then, E_2 is a saddle. Otherwise, both two roots are negative under the conditions (4)–(6); then, E_2 is a stable node or focus. □

Theorem 4. The interior equilibrium $E_1^*\left(x_1^*, y_1^*\right)$ is a saddle when it exists and $x_1^* > m + \sqrt{a}$. As for $x_1^* < m + \sqrt{a}$, E_1^* is a locally asymptotically stable equilibrium when $a_{11}\left(x_1^*, y_1^*\right) < 0$, while E_1^* is an unstable node or focus when $a_{11}\left(x_1^*, y_1^*\right) > 0$. The other interior equilibrium $E_2^*\left(x_2^*, y_2^*\right)$ is a saddle whenever it exists.

Proof. The Jacobian matrix of model (1.3) evaluated at the equilibrium E_i^* $(i = 1, 2)$ can be written as follows:

$$J_{E_i^*\left(x_i^*, y_i^*\right)} = \begin{pmatrix} -\frac{3r}{nk}x_i^{*2} + 2r\left(\frac{1}{n} + \frac{1}{k}\right)x_i^* - r + \frac{y_i^*\left(m^2 - 2mx_i^* + x_i^{*2} - a\right)}{\left[\left(x_i^* - m\right)^2 + b\left(x_i^* - m\right) + a\right]^2} - e_1 & -\frac{d+e_2}{\beta} \\ -\beta\frac{y_i^*\left(m^2 - 2mx_i^* + x_i^{*2} - a\right)}{\left[\left(x_i^* - m\right)^2 + b\left(x_i^* - m\right) + a\right]^2} & 0 \end{pmatrix};$$

then the trace and the determinant of the Jacobian matrix can be written as follows:

$$Tr\left(J_{E_i^*}\right) = a_{11}\left(x_i^*, y_i^*\right), \quad Det\left(J_{E_i^*}\right) = -\frac{y_i^*\left(m^2 - 2mx_i^* + x_i^{*2} - a\right)(d + e_2)}{\left[\left(x_i^* - m\right)^2 + b\left(x_i^* - m\right) + a\right]^2}.$$

The sign of $Tr\left(J_{E_i^*}\right)$ cannot be directly obtained since the expression is too complicated, while the sign for $Det\left(J_{E_i^*}\right)$ is determined by the relationship between the values of x_i^* and $m + \sqrt{a}$. It can be easily obtained that $Det\left(J_{E_1^*}\right) > 0$ when $x_1^* < m + \sqrt{a}$ and $Det\left(J_{E_1^*}\right) < 0$ when $x_1^* > m + \sqrt{a}$. Furthermore, the Jacobian matrix has two characteristic roots with opposite signs and E_1^* is a saddle as $x_1^* > m + \sqrt{a}$. As for $x_1^* < m + \sqrt{a}$ being satisfied, the Jacobian matrix has two negative characteristic roots and E_1^* is a locally asymptotically stable equilibrium when $a_{11}\left(x_1^*, y_1^*\right) < 0$, but the Jacobian matrix has two positive characteristic roots and E_1^* is an unstable node or focus when $a_{11}\left(x_1^*, y_1^*\right) > 0$. However, it can be easily judged that the sign of $Det\left(J_{E_2^*}\right)$ is negative under the necessary condition for the existence of E_2^*: $\beta > b(d + e_2)$. Thus, E_2^* is always a saddle whenever it exists. □

3. Analysis of harvesting

In this section, we will investigate the existence of an economic equilibrium and discuss the maximum sustainable total yield (MSTY) problem in model (1.3).

3.1. Economic equilibrium

The economic equilibrium can be obtained by the definition of $TC = TR$, where TC represents the cost for harvesting and TR refers to the full economic return on the obtained through harvesting. It is of great significance to study the existence of economic equilibria since the total profit is directly determined by the relationship between TC and TR. Let c_1 and c_2 represent the cost of unit effort e_1 and e_2, respectively. Let p_1 represent the sum of the direct economic value generated by the comprehensive utilization of cyanobacteria per unit and the indirect economic value generated by the environmental quality improvement brought by harvesting cyanobacteria per unit. p_2 represents the economic benifit of unit population of fish. Then we have the following theorem.

Theorem 5. Model (1.3) has a non-trivial economic equilibrium when harvesting cyanobacteria and fish is profitable and the following condition is satisfied.

$$\frac{rc_1p_2\left(kp_1-c_1\right)\left(c_1-np_1\right)}{knc_2p_1^3} > \frac{c_2p_1\left(c_1-mp_1\right)}{p_2\left[ap_1^2+bp_1\left(c_1-mp_1\right)+\left(c_1-mp_1\right)^2\right]} > \frac{d}{\beta}.$$

Proof. The possible economic equilibria are determined by the following equations:

$$\begin{cases} rx\left(1-\dfrac{x}{k}\right)\left(\dfrac{x}{n}-1\right)-\dfrac{(x-m)\,y}{a+b\,(x-m)+(x-m)^2}-e_1x=0,\\ \beta\dfrac{(x-m)\,y}{a+b\,(x-m)+(x-m)^2}-dy-e_2y=0,\\ S=(p_1x-c_1)\,e_1+(p_2y-c_2)\,e_2=0. \end{cases}$$

From the above equations, we can obtain

$$\begin{aligned} &x_\infty=\frac{c_1}{p_1},\ \ y_\infty=\frac{c_2}{p_2},\\ &e_{1\infty}=r\left(1-\frac{x_\infty}{k}\right)\left(\frac{x_\infty}{n}-1\right)-\frac{(x_\infty-m)\,y_\infty}{\left[a+b\,(x_\infty-m)+(x_\infty-m)^2\right]x_\infty},\\ &e_{2\infty}=\beta\frac{x_\infty-m}{a+b\,(x_\infty-m)+(x_\infty-m)^2}-d, \end{aligned}$$

and the efforts are positive when the above condition is satisfied; therefore, there exists a non-trival econimic equilibrium $(x_\infty, y_\infty, e_{1\infty}, e_{2\infty})$ in model (1.3). □

3.2. Maximum sustainable total yield

For a multi-species model with several harvesting terms, we always tend to gain the MSTY [30,31], which is the maximum biomass of total harvested populations and it varies with harvesting efforts

under the premise of ensuring that all species can survive continuously. It is necessary to ensure the persistence of the populations; however, interior equilibrium E_2^* is a saddle whenever it exists; thus, we analyze the existence of the MSTY in model (1.3) at interior equilibrium E_1^*. The expression of the total yield function at E_1^* can be written as follows:

$$Y(e_1, e_2) = e_1 x_1^* + e_2 y_2^* = e_1 x_1^* + \frac{e_2\left[a + b\left(x_1^* - m\right) + \left(x_1^* - m\right)^2\right]\left[r x_1^*\left(1 - \frac{x_1^*}{k}\right)\left(\frac{x_1^*}{n} - 1\right) - e_1 x_1^*\right]}{x_1^* - m}.$$

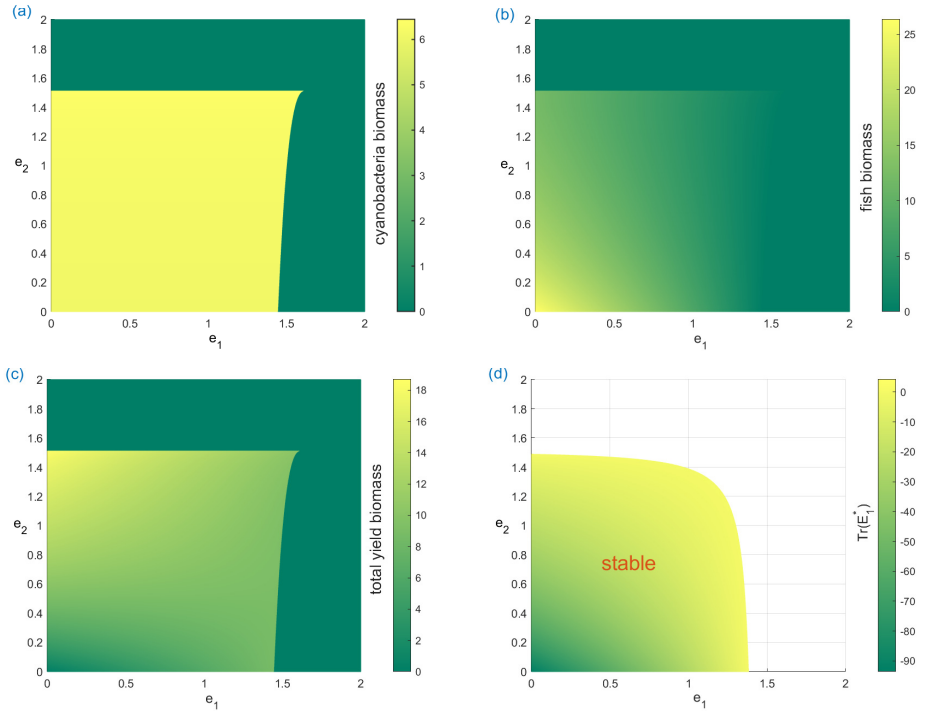

Figure 1. (a) The biomass of prey at E_1^* with varying harvesting efforts. (b) The biomass of the predator at E_1^* with varying harvesting efforts. (c) The total yield biomass of predator and prey at E_1^* with varying harvesting efforts. (d) The stable area of interior equilibrium E_1^*; in this area $Det\left(E_1^*\right)$ is always positive.

The two efforts of harvesting e_1^* and e_2^* should satisfy

$$\left.\frac{\partial Y(e_1, e_2)}{\partial e_1}\right|_{(e_1^*, e_2^*)} = \left.\frac{\partial Y(e_1, e_2)}{\partial e_2}\right|_{(e_1^*, e_2^*)} = 0,$$

or that $Y\left(e_1^*, e_2^*\right)$ is the nondifferentiable point of function $Y(e_1, e_2)$ when the MSTY exists. It is obvious that $Y(e_1, e_2)$ is a linear function with respect to e_1, which means that $\partial^2 Y(e_1, e_2)/\partial e_1^2 = 0$. Therefore, we cannot directly tell the exsitence of the MSTY through the Hessian matrix. We give a numerical simulation since the expression of the yield function is too complex to analyze, and the values are taken as follows:

$$k = 100,\ n = 3,\ m = 6,\ \beta = 3,\ r = 1.5,\ d = 1,\ a = 0.2,\ b = 0.3.$$

The biomasses of prey and predator at equilibrium E_1^* and the total yield for various harvesting efforts e_1 and e_2 are shown as Figure 1. It can be seen in Figure 1(a) that the influences of e_1 and e_2 on the biomass of cyanobacteria at E_1^* are very small initially, but that cyanobacteria will become extinct when $e_2 > 1.5117$ or fish is extinct. With the increase of the harvesting efforts e_1 and e_2, the biomass of fish at E_1^* gradually decreases and tends to become extinct, as is shown in Figure 1(b). From Figure 1(c), we can get that the total yield biomass reaches the maximum at the nondifferentiable point $(0, 1.5117, 18.7706)$. However, the interior equilibrium E_1^* is unstable at this point according to Figure 1(d), which implies that there is no MSTY in model (1.3). We always harvest both cyanobacteria and fish at different efforts in real life. Moreover, we study the MSTY problem of model (1.3) when the two harvesting efforts are in a certain proportion. Assume that the harvesting efforts $e_1 = \lambda e_2$. In this paper, we assume that the harvesting efforts of humans on both the cyanobacteria and fish populations are non-zero. Therefore, $\lambda \neq 0$ here. As a result, the total yield function can be expressed as follows:

$$H(e) = Y\left(e, \frac{e}{\lambda}\right).$$

Let us take a different value of λ and analyze it by numerical simulations. It can be seen in Figure 2 that with the increase of harvesting effort e, the fish population decreases sharply and tends to be extinct at E_1^*, while the cyanobacteria population keep steady; and, the total yield biomass increases first and then changes smoothly, and the interior equilibrium E_1^* disappears with the extinction of fish finally. In addition, the solid line in Figure 2 indicates stability and the dashed line indicates instability based on Theorem 4. The total yield function reaches its sustainable maximum at $H(1.0389) = 10.8641$ when $\lambda = 1$, and at $H(1.2701) = 9.2723$ when $\lambda = 2$.

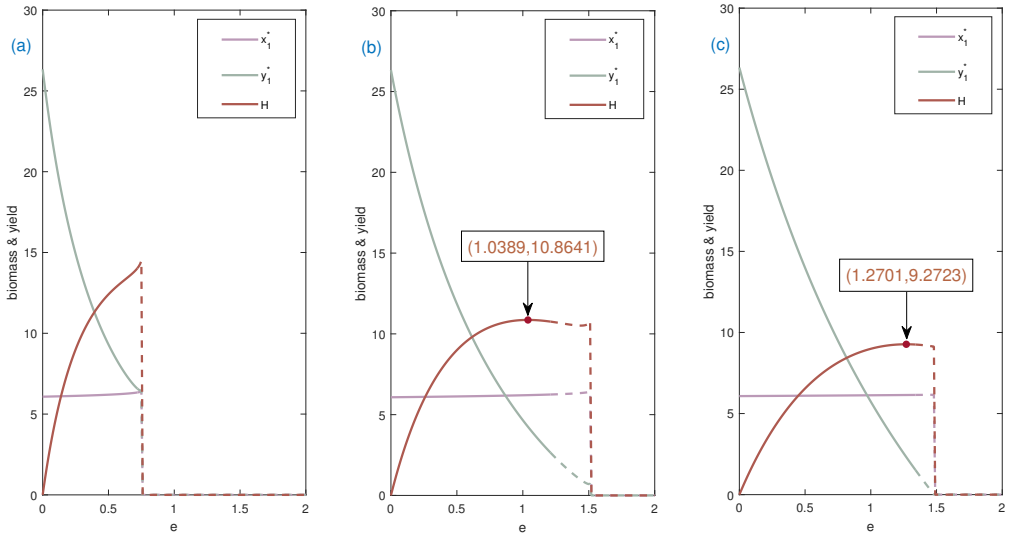

Figure 2. The population densities and total yield biomass $H(e)$ with varying harvesting efforts at E_1^*. (a) $\lambda = 0.5$. (b) $\lambda = 1$. (c) $\lambda = 2$.

4. Local bifurcation

In this section, we will discuss the local bifurcation in model (1.3) theoretically. We take the aggregration parameter m and harvesting efforts e_1 and e_2 as the bifurcation parameters; transcritical bifurcation, saddle-node bifurcation and Hopf bifurcation with codimension 1 and Bogdanov-Takens bifurcation with codimension 2 are analyzed successively.

4.1. Transcritical bifurcation

Transcritical bifurcation always occurs at the boundary equilibria; since the equilibrium E_1 is unstable whenever it exists, transcritical bifurcation will only happen at E_2. The transcritical bifurcations are caused by the collisions of interior equilibria E_1^* or E_2^* with E_2, so we choose aggregration parameter m as the bifurcation parameter; then, we can obtain the expressions of the critical value correspondingly

$$m_1 = \frac{b+k+n}{2} + \frac{\sqrt{\Delta_1}}{2r} + \frac{\sqrt{\Delta_2}-\beta}{2\left(d+e_2\right)}, \quad m_2 = \frac{b+k+n}{2} + \frac{\sqrt{\Delta_1}}{2r} - \frac{\sqrt{\Delta_2}+\beta}{2\left(d+e_2\right)}.$$

Then, if m_1 or m_2 are in the set $[0,k]$, the predator-free equilibrium E_2 will translate its stability as the value of parameter m passes through m_1 or m_2.

Theorem 6. The model (1.3) will undergo a transcritical bifurcation at the equilibrium E_2 when $m = m_1 \in [0,k]$ or $m = m_2 \in [0,k]$ and

$$kr + nr + \sqrt{r^2(k-n)^2 - 4re_1nk} - 2rm_{1\ or\ 2} \neq 0, 2r\sqrt{a}, \frac{2r(k+n) + -\sqrt{4r^2(k+n)^2 - 12rkn(r+e_1)}}{3}.$$

Proof. When $m = m_1 \in [0,k]$, the elements of Jacobian matrix $J_{(E_2;m_1)}$ are

$$a_{11}\left(x_2,0\right), \quad a_{12}\left(x_2\right)|_{m=m_1}, \quad a_{21}\left(x_2,0\right) = a_{22}\left(x_2\right)|_{m=m_1} = 0,$$

letting V and W are eigenvectors of zero eigenvalues of $J_{(E_2;m_1)}$ and $J^T_{(E_2;m_1)}$ respectively. Without loss of generality, we can take

$$V = \begin{pmatrix} v_1 \\ v_2 \end{pmatrix} = \begin{pmatrix} -a_{12}\left(x_2\right)|_{m=m_1} \\ a_{11}\left(x_2,0\right) \end{pmatrix}, \quad W = \begin{pmatrix} w_1 \\ w_2 \end{pmatrix} = \begin{pmatrix} 0 \\ 1 \end{pmatrix};$$

then

$$W^T F_m\left(E_2;m_1\right) = \begin{pmatrix} 0 & 1 \end{pmatrix} \left.\begin{pmatrix} -\frac{y\left[(x-m)^2-a\right]}{\left[a+b(x-m)+(x-m)^2\right]^2} \\ \frac{\beta y\left[(x-m)^2-a\right]}{\left[a+b(x-m)+(x-m)^2\right]^2} \end{pmatrix}\right|_{(E_2;m_1)} = \begin{pmatrix} 0 & 1 \end{pmatrix} \begin{pmatrix} 0 \\ 0 \end{pmatrix} = 0,$$

$$W^T\left[DF_m\left(E_2;m_1\right)V\right] = \begin{pmatrix} 0 & 1 \end{pmatrix} \left.\begin{pmatrix} 0 & -\frac{(x-m)^2-a}{\left[a+b(x-m)+(x-m)^2\right]^2} \\ 0 & \frac{\beta\left[(x-m)^2-a\right]}{\left[a+b(x-m)+(x-m)^2\right]^2} \end{pmatrix}\right|_{(E_2;m_1)} \begin{pmatrix} -a_{12}\left(x_2\right)|_{m=m_1} \\ a_{11}\left(x_2,0\right) \end{pmatrix}$$

$$= \left.\frac{a_{11}\left(x,y\right)\beta\left[(x-m)^2-a\right]}{\left[a+b\left(x-m\right)+\left(x-m\right)^2\right]^2}\right|_{(E_2;m_1)},$$

$$W^T\left[D^2F_m(E_2;m_1)(V,V)\right]=\begin{pmatrix} w_1 & w_2 \end{pmatrix}\begin{pmatrix} g^1_{xx} & g^1_{xy} & g^1_{yx} & g^1_{yy} \\ g^2_{xx} & g^2_{xy} & g^2_{yx} & g^2_{yy} \end{pmatrix}\Bigg|_{(E_2;m_1)}\begin{pmatrix} v_1v_1 \\ v_1v_2 \\ v_2v_1 \\ v_2v_2 \end{pmatrix}$$
$$=\frac{2\beta\left[a-(x_2-m_1)^2\right]\left[3rx_2^2-2r(k+n)x_2+kn(r+e_1)\right](m_1-x_2)}{nk\left[a+b(x_2-m_1)+(x_2-m_1)^2\right]^3}.$$

It can be easily verified that the following inequalities hold when the conditions given by the theorem are satisfied:

$$W^T\left[DF_m(E_2;m_1)V\right]\neq 0,\quad W^T\left[D^2F_m(E_2;m_1)(V,V)\right]\neq 0,$$

which means that the model (1.3) undergoes a transcritical bifurcation at equilibrium E_2 according to Sotomayor's theorem [32].

The proof process of the theorem when $m=m_2\in[0,k]$ is omitted since it is similar to the above. □

4.2. Saddle-node bifurcation

On the basis of the previous analysis of the existence of the equilibria and some appropriate conditions, it is obvious that the predator-free equilibria E_1 and E_2 will overlap as an equilibrium $E_{sn}(x_{sn},y_{sn})$ when $\Delta_1=0$, and the interior equilibria will also overlap as an equilibrium $E^*_{sn}(x^*_{sn},y^*_{sn})$ when $\Delta_2=0$. These dynamic phenomena are caused by two saddle-node bifurcations; then, we have the following two theorems.

Theorem 7. Model (1.3) will undergo a saddle-node bifurcation at the equilibrium $E_{sn}(x_{sn},y_{sn})$ with respect to e_1 as the bifurcation parameter when the parameters satisfy the following two conditions:

(1) $2m<k+n$,

(2) $e_1=e_{1sn}=\frac{r(k-n)^2}{4nk}$.

Proof. Now we verify the transversality condition for the occurrence of saddle-node bifurcation at $e_1=e_{1sn}$ using Sotomayor's theorem. The equilibrium E_{sn} exists under the conditions (1) and (2) according to the previous analysis; the Jacobian matrix at E_{sn} can be written as

$$J_{E_{sn}}=\begin{pmatrix} 0 & -\frac{x_{sn}-m}{(x_{sn}-m)^2+b(x_{sn}-m)+a} \\ 0 & \frac{\beta(x_{sn}-m)}{(x_{sn}-m)^2+b(x_{sn}-m)+a}-d-e_2 \end{pmatrix},$$

where $x_{sn}=\frac{k+n}{2}$, corresponding to $y_{sn}=0$. It is obvious that $Det(J_{E_{sn}})=0$ such that zero is one of the eigenvalues of $J_{E_{Sn}}$. Letting V and W represent eigenvectors corresponding to the eigenvalue zero for the matrices $J_{E_{sn}}$ and $J^T_{E_{sn}}$. Assuming that the equilibrium E_{sn} does not coincide with E^*_1 or E^*_2 such that $f(x_{sn})\neq 0$, then without loss of generality, we can take

$$V=\begin{pmatrix} v_1 \\ v_2 \end{pmatrix}=\begin{pmatrix} 1 \\ 0 \end{pmatrix},\quad W=\begin{pmatrix} w_1 \\ w_2 \end{pmatrix}=\begin{pmatrix} 1 \\ \frac{x_{sn}-m}{f(x_{sn})} \end{pmatrix}$$

such that

$$W^TF_{e_1}(E_{sn};e_{1sn})=\begin{pmatrix} w_1 & w_2 \end{pmatrix}\begin{pmatrix} -x_{sn} \\ 0 \end{pmatrix}=-x_{sn}\neq 0,$$

$$W^T\left[D^2F_{e_1}(E_{sn};e_{1sn})(V,V)\right]=\begin{pmatrix} w_1 & w_2\end{pmatrix}\begin{pmatrix} g^1_{xx} & g^1_{xy} & g^1_{yx} & g^1_{yy}\\ g^2_{xx} & g^2_{xy} & g^2_{yx} & g^2_{yy}\end{pmatrix}\Big|_{(E_{sn};e_{1sn})}\begin{pmatrix} v_1v_1\\ v_1v_2\\ v_2v_1\\ v_2v_2\end{pmatrix}$$

$$=-\frac{r(k+n)}{kn}\neq 0.$$

Hence the eigenvectors V and W satisfy the transversality conditions such that model (1.3) has a saddle-node bifurcation at E_{sn} when $e_1=e_{1sn}$. □

Theorem 8. Model (1.3) will undergo a saddle-node bifurcation at the equilibrium $E^*_{sn}(x^*_{sn},y^*_{sn})$ with respect to e_2 as the bifurcation parameter when the parameters satisfy the following three conditions:

(1) $\beta>b(d+e_2)$,

(2) $e_2=e_{2sn}=\frac{\beta}{2\sqrt{a}+b}-d>0$,

(3) $\left(2mr+2r\sqrt{a}-kr-nr\right)^2<\Delta_1$.

Proof. Similiar to the proof process for the above theorem, we need to verify the transversality condition for the occurrence of saddle-node bifurcation at $e_2=e_{2sn}$. The interior equilibrium $E^*_{sn}(x^*_{sn},y^*_{sn})$ exists under the above three conditions according to the previous analysis of equilibria, where

$$x^*_{sn}=m+\sqrt{a},\ \ y^*_{sn}=\left(2\sqrt{a}+b\right)\left[rx^*_{sn}\left(1-\frac{x^*_{sn}}{k}\right)\left(\frac{x^*_{sn}}{n}-1\right)-e_1x^*_{sn}\right],$$

and the Jacobian matrix at E^*_{sn} can be written as

$$J_{E^*_{sn}}=\begin{pmatrix} a_{11}(x^*_{sn},y^*_{sn}) & -\frac{1}{b+2\sqrt{a}}\\ 0 & 0\end{pmatrix}.$$

Letting V and W represent eigenvectors corresponding to the eigenvalue zero for the matrices $J_{E^*_{sn}}$ and $J^{*T}_{E^*_{sn}}$, and without loss of generality, we can take

$$V=\begin{pmatrix} v_1\\ v_2\end{pmatrix}=\begin{pmatrix} \frac{1}{b+2\sqrt{a}}\\ a_{11}(x^*_{sn},y^*_{sn})\end{pmatrix},\ \ W=\begin{pmatrix} w_1\\ w_2\end{pmatrix}=\begin{pmatrix} 0\\ 1\end{pmatrix};$$

hence

$$W^TF_{e_2}(E^*_{sn};e_{2sn})=\begin{pmatrix} w_1 & w_2\end{pmatrix}\begin{pmatrix} 0\\ -y^*_{sn}\end{pmatrix}=-y^*_{sn}\neq 0,$$

$$W^T\left[D^2F_{e_2}(E^*_{sn};e_{2sn})(V,V)\right]=\begin{pmatrix} w_1 & w_2\end{pmatrix}\begin{pmatrix} g^1_{xx} & g^1_{xy} & g^1_{yx} & g^1_{yy}\\ g^2_{xx} & g^2_{xy} & g^2_{yx} & g^2_{yy}\end{pmatrix}\Big|_{(E^*_{sn};e_{2sn})}\begin{pmatrix} v_1v_1\\ v_1v_2\\ v_2v_1\\ v_2v_2\end{pmatrix}$$

$$=-\frac{2\beta y^*_{sn}}{\sqrt{a}\left(b+2\sqrt{a}\right)^4}\neq 0.$$

Therefore, the eigenvectors V and W satisfy the transversality conditions for the occurrence of saddle-node bifurcation at the interior equilibrium E^*_{sn} when $e_2=e_{2sn}$. In addition, as the value of e_2 passes through e_{2sn}, there is an interior equilibrium in model (1.3) and then it becomes two. □

4.3. Hopf bifurcation

In this subsection, we concentrate on the occurrence of Hopf bifurcation at the interior equilibrium E_1^* of model (1.3) based on the previous discussion about the stability of the interior equilibria.

In order to study Hopf bifurcation in model (1.3), we take harvesting effort e_1 as the bifurcation parameter, and we require that $e_1 = e_{1hp}$ is a positive root of $a_{11}\left(x_1^*, y_1^*\right) = 0$. The stability of the interior equilibrium E_1^* changes when e_1 passes through e_{1hp}; then, we obtain the following theorem.

Theorem 9. Model (1.3) will undergo a Hopf bifurcation at the interior equilibrium $E_1^*\left(x_1^*, y_1^*\right)$ when $e_1 = e_{1hp}$ and the other parameters satisfy the following three conditions:

(1) $\Delta_1 > 0$,
(2) $\Delta_2 > 0$,
(3) $\max\{m, x_1\} < x_1^* < \min\left\{m + \sqrt{a}, x_2, k\right\}$,
(4) $a < m^2$.

Proof. It is easy to testify that the interior equilibrium E_1^* exists and $Det\left(J_{E_1^*}\right)|_{e_1=e_{1hp}} > 0$ is satisfied under the conditions (1)–(3). Since we have the set $a_{11}\left(x_1^*, y_1^*\right)|_{e_1=e_{1hp}} = 0$, i.e. the trace of $J_{E_1^*}$ is zero, we only need to verify the transversality condition for Hopf bifurcation. It can be easily obtained that

$$\frac{d}{de_1} Tr\left(J_{E_1^*}\right)\Big|_{e_1=e_{1hp}} = \frac{-2x_1^{*3} + (5m-b)\,x_1^{*2} + 2m\,(b-2m)\,x_1^* + m\left(m^2 - bm + a\right)}{\left(x_1^* - m\right)^3 + b\left(x_1^* - m\right)^2 + a\left(x_1^* - m\right)}.$$

Since the inequality $\frac{d}{de_1} Tr\left(J_{E_1^*}\right)\Big|_{e_1=e_{1hp}} > 0$ holds under the condition (4), the transversality condition for Hopf bifurcation is satisfied.

The first Lyapunov coefficient l_1 in Hopf bifurcation determines the stability of the limit cycle that emerges from a bifurcation of an equilibrium. A positive value for the coefficient indicates an unstable limit cycle, while a negative value indicates a stable limit cycle. In order to evaluate the stability of the limit cycle after Hopf bifurcation at interior equilibrium E_1^*, we calculate the first Lyapunov number l_1 at the equilibrium E_1^* of model (1.3) using the method described in [33, 34]. First, translate E_1^* into the origin $(0, 0)$, letting $x^* = x - x_1^*$ and $y^* = y - y_1^*$; then, model (1.3) can be expressed as

$$\begin{cases} \dot{x^*} = \alpha_{10}x^* + \alpha_{01}y^* + \alpha_{20}x^{*2} + \alpha_{11}x^*y^* + \alpha_{02}y^{*2} + \alpha_{30}x^{*3} + \alpha_{21}x^{*2}y^* + \alpha_{12}x^*y^{*2} + \alpha_{03}y^{*3} + P_1, \\ \dot{y^*} = \beta_{10}x^* + \beta_{01}y^* + \beta_{20}x^{*2} + \beta_{11}x^*y^* + \beta_{02}y^{*2} + \beta_{30}x^{*3} + \beta_{21}x^{*2}y^* + \beta_{12}x^*y^{*2} + \beta_{03}y^{*3} + +P_2. \end{cases}$$

According to the previous content, we can obtain that $Tr\left(J_{E_1^*}\right) = \alpha_{10} + \beta_{01} = 0$ and $Det\left(J_{E_1^*}\right) = \alpha_{10}\beta_{01} - \alpha_{01}\beta_{10} > 0$; the other parameters α_{ij} and β_{ij} can be seen in Appendix A. P_1 and P_2 are the remainder terms in the Taylor series of $\dot{x^*}$ and $\dot{y^*}$. The first Lyapunov number l_1 can be expressed as follows:

$$\begin{aligned} l_1 = & \frac{-3\pi}{2\alpha_{01}Det\left(J_{E_1^*}\right)^{3/2}} \Big\{\Big[\alpha_{10}\beta_{10}(\alpha_{11}^2 + \alpha_{11}\beta_{02} + \alpha_{02}\beta_{11}) + \alpha_{10}\alpha_{01}(\beta_{11}^2 + \alpha_{20}\beta_{11} + \alpha_{11}\beta_{02}) \\ & - 2\alpha_{10}\beta_{10}(\beta_{02}^2 - \alpha_{20}\alpha_{02}) - 2\alpha_{10}\alpha_{01}(\alpha_{20}^2 - \beta_{20}\beta_{02}) - \alpha_{01}^2(2\alpha_{20}\beta_{20} + \beta_{11}\beta_{20}) \\ & + (\alpha_{01}\beta_{10} - 2\alpha_{10}^2)(\beta_{11}\beta_{02} - \alpha_{11}\alpha_{20}) + \beta_{10}^2(\alpha_{11}\alpha_{02} + 2\alpha_{02}\beta_{02})\Big] \end{aligned}$$

$$-(\alpha_{10}^2+\alpha_{01}\beta_{10})\left[3(\beta_{10}\beta_{03}-\alpha_{01}\alpha_{30})+2\alpha_{10}(\alpha_{21}+\beta_{12})+(\beta_{10}\alpha_{12}-\alpha_{01}\beta_{21})\right]\Big\},$$

$$=\frac{-3\pi}{2\sqrt{-\alpha_{01}^3\beta_{10}}}\left(\alpha_{11}\alpha_{20}-3\alpha_{01}\alpha_{30}-\alpha_{01}\beta_{21}\right).$$

Furthermore, when $e_1 = e_{1hp}$, model (1.3) will undergo a supercritical Hopf bifurcation at the interior equilibrium E_1^* if $l_1 < 0$, but the Hopf bifurcation is subcritical if $l_1 > 0$. Because the expression of l_1 is too cumbersome to determine the sign of it, we will give a numerical example in the next section to increase its reliability. □

4.4. Bogdanov-Takens bifurcation

It is necessary for us to investigate the joint influence of e_1 and e_2 on model (1.3) since the harvesting efforts of cyanobacteria and fish are not always constant in real life. In this subsection, we select e_1 and e_2 as Bogdanov-Takens bifurcation parameters to study the influence on the dynamic behavior caused by the harvesting efforts theoretically.

Theorem 10. When e_1 and e_2 are selected as the bifurcation parameters for model (1.3), a Bogdanov-Takens bifurcation will occur at the point (e_{1bt}, e_{2bt}), provided that the two harvesting efforts e_{1bt} and e_{2bt} satisfy the following two conditions:

$$Det\left(J_{E_1^*}\right)|_{(e_{1bt},e_{2bt})}=0,\quad Tr\left(J_{E_1^*}\right)|_{(e_{1bt},e_{2bt})}=0.$$

Proof. In order to analyze the dynamic behavior of model (1.3) within a small range of the Bogdanov-Takens point, we first calculate the local expressions of saddle-node bifurcation, Hopf bifurcation and homoclinic bifurcation by translating model (1.3) into a normal form.

For harvesting efforts, we introduce two small disturbances ξ_1 and ξ_2, i.e., substituting $e_1 = e_{1bt}+\xi_1$ and $e_1 = e_{2bt}+\xi_2$ in model (1.3); then, we get

$$\begin{cases}\dfrac{dx}{dt}=rx\left(1-\dfrac{x}{k}\right)\left(\dfrac{x}{n}-1\right)-\dfrac{(x-m)\,y}{a+b\,(x-m)+(x-m)^2}-(e_{1bt}+\xi_1)\,x,\\[2ex] \dfrac{dy}{dt}=\beta\dfrac{(x-m)\,y}{a+b\,(x-m)+(x-m)^2}-dy-(e_{2bt}+\xi_2)\,y.\end{cases}\tag{4.1}$$

After taking the variable substitutions $u_1 = x - x_1^*$ and $u_2 = y - y_1^*$, the equilibrium E_1^* comes to the origin, and model (4.1) becomes

$$\begin{cases}\dfrac{du_1}{dt}=p_{00}\,(\xi_1,\xi_2)+p_{10}\,(\xi_1,\xi_2)\,u_1+\alpha_{01}u_2+\alpha_{20}u_1^2+\alpha_{11}u_1u_2+\alpha_{02}u_2^2+P_3,\\[2ex] \dfrac{du_2}{dt}=q_{00}\,(\xi_1,\xi_2)+\beta_{10}u_1+q_{01}\,(\xi_1,\xi_2)\,u_2+\beta_{20}u_1^2+\beta_{11}u_1u_2+\beta_{02}u_2^2+P_4,\end{cases}\tag{4.2}$$

where $p_{00}\,(\xi_1,\xi_2) = -\xi_1 x_1^*$, $p_{10}\,(\xi_1,\xi_2) = -\xi_1$, $q_{00}\,(\xi_1,\xi_2) = -\xi_2 y_1^*$ and $q_{01}\,(\xi_1,\xi_2) = -\xi_2$, and the other parameters α_{ij} and β_{ij} are consistent with the previous respective definitions. Besides, P_3 and P_4 are the remainder terms in the Taylor series of $\frac{du_1}{dt}$ and $\frac{du_2}{dt}$ respectively in model (4.2).

Then we substitute the variables in model (4.2) near the origin as follows:

$$v_1 = u_1,\quad v_2 = p_{00}\,(\xi_1,\xi_2)+p_{10}\,(\xi_1,\xi_2)\,u_1+\alpha_{01}u_2+\alpha_{20}u_1^2+\alpha_{11}u_1u_2+\alpha_{02}u_2^2+P_3;$$

under the substitutions, model (4.2) becomes

$$\begin{cases} \dfrac{dv_1}{dt} = v_2, \\ \dfrac{dv_2}{dt} = c_{00}(\xi_1,\xi_2) + c_{10}(\xi_1,\xi_2)\, v_1 + c_{01}(\xi_1,\xi_2)\, v_2 + c_{20}(\xi_1,\xi_2)\, v_1^2 + c_{11}(\xi_1,\xi_2)\, v_1 v_2 \\ \qquad + c_{02}(\xi_1,\xi_2)\, v_2^2 + P_5, \end{cases} \tag{4.3}$$

where the expressions of c_{ij} can be seen in Appendix B and P_5 is the remainder term in the Taylor series of $\frac{dv_2}{dt}$ in model (4.3).

A new time variable τ is introduced to further transform model (4.3) into the normal form such that $(1 - c_{02}(\xi)\, v_1)\, d\tau = dt$. We rewrite t to denote τ for simplicity. Then, under the change of $w_1 = v_1$ and $w_2 = v_2\,(1 - c_{02} v_1)$, model (4.3) becomes

$$\begin{cases} \dfrac{dw_1}{dt} = w_2, \\ \dfrac{dw_2}{dt} = \theta_{00}(\xi_1,\xi_2) + \theta_{10}(\xi_1,\xi_2)\, w_1 + \theta_{01}(\xi_1,\xi_2)\, w_2 + \theta_{20}(\xi_1,\xi_2)\, w_1^2 + \theta_{11}(\xi_1,\xi_2)\, w_1 w_2 + P_6, \end{cases} \tag{4.4}$$

where

$$\theta_{00}(\xi_1,\xi_2) = c_{00}(\xi_1,\xi_2), \quad \theta_{10}(\xi_1,\xi_2) = c_{10}(\xi_1,\xi_2) - 2c_{00}(\xi_1,\xi_2)\, c_{02}(\xi_1,\xi_2), \quad \theta_{01}(\xi_1,\xi_2) = c_{01}(\xi_1,\xi_2),$$
$$\theta_{20}(\xi_1,\xi_2) = c_{20}(\xi_1,\xi_2) - 2c_{10}(\xi_1,\xi_2)\, c_{02}(\xi_1,\xi_2) + c_{00}(\xi_1,\xi_2)\, c_{02}^2(\xi_1,\xi_2),$$
$$\theta_{11}(\xi_1,\xi_2) = c_{11}(\xi_1,\xi_2) - 2c_{01}(\xi_1,\xi_2)\, c_{02}(\xi_1,\xi_2),$$

and P_6 is the remainder term in the Taylor series of $\frac{dw_2}{dt}$ in model (4.4).

Assuming that $\theta_{20}(\xi_1,\xi_2) \neq 0$, we define $z_1 = w_1 + \frac{\theta_{10}(\xi_1,\xi_2)}{2\theta_{20}(\xi_1,\xi_2)}$, $z_2 = w_2$. As a result, model (4.4) takes on the following new form:

$$\begin{cases} \dfrac{dz_1}{dt} = z_2, \\ \dfrac{dz_2}{dt} = \sigma_{00}(\xi_1,\xi_2) + \sigma_{01}(\xi_1,\xi_2)\, z_2 + \sigma_{20}(\xi_1,\xi_2)\, z_1^2 + \sigma_{11}(\xi_1,\xi_2)\, z_1 z_2 + P_7, \end{cases} \tag{4.5}$$

where

$$\sigma_{00}(\xi_1,\xi_2) = \theta_{00}(\xi_1,\xi_2) - \frac{\theta_{10}^2(\xi_1,\xi_2)}{4\theta_{20}(\xi_1,\xi_2)}, \quad \sigma_{01}(\xi_1,\xi_2) = \theta_{01}(\xi_1,\xi_2) - \frac{\theta_{10}(\xi_1,\xi_2)\,\theta_{11}(\xi_1,\xi_2)}{2\theta_{20}(\xi_1,\xi_2)},$$
$$\sigma_{20}(\xi_1,\xi_2) = \theta_{20}(\xi_1,\xi_2), \quad \sigma_{11}(\xi_1,\xi_2) = \theta_{11}(\xi_1,\xi_2),$$

and P_7 is the remainder term in the Taylor series of $\frac{dz_2}{dt}$ in model (4.5).

In order to simplify the coefficient of term $\sigma_{20}(\xi_1,\xi_2)\, z_1^2$ in model (4.5), we let

$$s_1 = z_1, \quad s_2 = \frac{z_2}{\sqrt{|\sigma_{20}(\xi_1,\xi_2)|}}, \quad \tau = t\sqrt{|\sigma_{20}(\xi_1,\xi_2)|};$$

rewriting t to denote τ, then model (4.5) has a new form:

$$\begin{cases} \dfrac{ds_1}{dt} = s_2, \\ \dfrac{ds_2}{dt} = \gamma_{00}(\xi_1,\xi_2) + \gamma_{01}(\xi_1,\xi_2)\, s_2 + \gamma_{20}(\xi_1,\xi_2)\, s_1^2 + \gamma_{11}(\xi_1,\xi_2)\, s_1 s_2 + P_8, \end{cases} \tag{4.6}$$

where

$$\gamma_{00}(\xi_1,\xi_2)=\frac{\sigma_{00}(\xi_1,\xi_2)}{|\sigma_{20}(\xi_1,\xi_2)|},\ \ \gamma_{01}(\xi_1,\xi_2)=\frac{\sigma_{01}(\xi_1,\xi_2)}{\sqrt{|\sigma_{20}(\xi_1,\xi_2)|}},$$
$$\gamma_{20}(\xi_1,\xi_2)=\frac{\sigma_{20}(\xi_1,\xi_2)}{|\sigma_{20}(\xi_1,\xi_2)|},\ \ \gamma_{11}(\xi_1,\xi_2)=\frac{\sigma_{11}(\xi_1,\xi_2)}{\sqrt{|\sigma_{20}(\xi_1,\xi_2)|}},$$

and P_8 is the remainder term in the Taylor series of $\frac{ds_2}{dt}$ in model (4.6).

Supposing that $\sigma_{11}\neq 0$, then $\gamma_{11}\neq 0$. Further setting

$$x=\frac{\sigma_{20}(\xi_1,\xi_2)}{|\sigma_{20}(\xi_1,\xi_2)|}\gamma_{11}^2(\xi_1,\xi_2)\,s_1,\ \ y=\gamma_{11}^3(\xi_1,\xi_2)\,s_2,\ \ \tau=\frac{\sigma_{20}(\xi_1,\xi_2)}{|\sigma_{20}(\xi_1,\xi_2)|\,\gamma_{11}(\xi_1,\xi_2)}t,$$

and rewriting t to denote τ, we obtain the normal form of model (4.1) at the Bogdanov-Takens point

$$\begin{cases}\dfrac{dx}{dt}=y,\\ \dfrac{dy}{dt}=\varpi_{00}(\xi_1,\xi_2)+\varpi_{01}(\xi_1,\xi_2)\,y+x^2+xy+P_9,\end{cases}\tag{4.7}$$

where

$$\varpi_{00}(\xi_1,\xi_2)=\frac{\sigma_{20}(\xi_1,\xi_2)}{|\sigma_{20}(\xi_1,\xi_2)|}\gamma_{00}(\xi_1,\xi_2)\,\gamma_{11}^4(\xi_1,\xi_2),\ \ \varpi_{01}(\xi_1,\xi_2)=\frac{\sigma_{20}(\xi_1,\xi_2)}{|\sigma_{20}(\xi_1,\xi_2)|}\gamma_{01}(\xi_1,\xi_2)\,\gamma_{11}(\xi_1,\xi_2),$$

and P_9 is the remainder term in the Taylor series of $\frac{d\varpi_2}{dt}$ in model (4.7).

Based on the results of [35], model (1.3) undergoes a Bogdanov-Takens bifurcation when $(e_1,e_2)=(e_{1bt},e_{2bt})$ and (ξ_1,ξ_2) is in a small domain of the origin. We obtain the local expressions of the following three bifurcation curves.

(1) The curve of saddle-node bifurcation:

$$SN=\{(\xi_1,\xi_2):\varpi_{00}(\xi_1,\xi_2)=0,\varpi_{01}(\xi_1,\xi_2)\neq 0\};$$

(2) The curve of Hopf bifurcation:

$$Hp=\left\{(\xi_1,\xi_2):\varpi_{01}(\xi_1,\xi_2)=\frac{\sigma_{20}(\xi_1,\xi_2)}{|\sigma_{20}(\xi_1,\xi_2)|}\sqrt{-\varpi_{00}(\xi_1,\xi_2)},\varpi_{00}(\xi_1,\xi_2)<0\right\};$$

(3) The curve of homoclinic bifurcation:

$$HL=\left\{(\xi_1,\xi_2):\varpi_{01}(\xi_1,\xi_2)=\frac{5\sigma_{20}(\xi_1,\xi_2)}{7\,|\sigma_{20}(\xi_1,\xi_2)|}\sqrt{-\varpi_{00}(\xi_1,\xi_2)},\varpi_{00}(\xi_1,\xi_2)<0\right\}.$$

□

5. Numerical simulation

Although we have obtained some theoretical results for model (1.3) in the previous sections, it is not easy to get intuitive knowledge about the dynamic behaviors of the model since some expressions in the theoretical analysis are truly complicated. Thus, we perform some precise numerical simulations to further research the model and investigate the dynamic behavior of it in this section. Throughout

the numerical simulations, we consider a set of hypothetical values of parameters according to their biological significance in model (1.3):

$$k = 50,\ n = 3,\ m = 30,\ \beta = 0.6,\ r = 1.5,\ d = 1,\ a = 0.02,\ b = 0.1.$$

Given these parameters, we can obtain the Hopf bifurcation curves of model (1.3) as Figure 3(a). Then, we fix the harvesting effort $e_1 = 3.194748196$, and let the other effort e_2 vary within a small range. We can get a bifurcation diagram of model (1.3) as Figure 3(b). Hopf bifurcation and saddle-node bifurcation occur when $e_2 = 0.5672232479$ and $e_2 = 0.5672232498$ respectively. The solid line in Figure 3(b) indicates stability and the dashed line indicates instability. Figure 4 reveals the detailed evolution process of Hopf bifurcation. The Bogdanov-Takens bifurcation parameters were

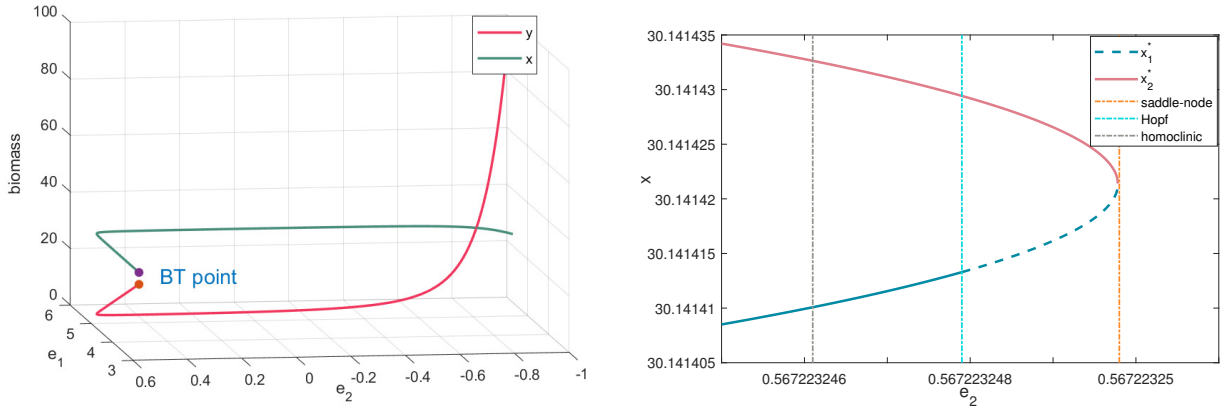

Figure 3. (a). Hopf bifurcation curves of model (1.3) given the previous parameters. (b). Bifurcation diagram of model (1.3) given the previous parameters and $e_1 = 3.174748196$.

calculated as $e_{1bt} = 3.194748196$ and $e_{2bt} = 0.5672232498$ on the premise of the above parameters. The biomasses of cyanobacteria at interior equilibria E_1^* and E_2^* with varying harvesting efforts are shown in Figure 5(a). Although it is not obvious, the curves lying on the curved surface of x_1^* in Figure 5(a) are saddle-node, Hopf and homoclinic bifurcation curves respectively. The projections of these curves on the $e_1 - e_2$ plane within a small range of (e_{1bt}, e_{2bt}) can be clearly seen in Figure 5(b). These bifurcation curves divide the left area of the Bogdanov-Takens bifurcation point in the $\xi_1 - \xi_2$ plane into four blocks named I, II, III and IV. Going through the SN curve top-down, one can observe an interior equilibrium that then evolves into two. There appears or disappears a periodic oscillation solution with the transform of the stability of interior equilibrium E_1^* when the parameters are located on the Hp curve. Along the HL curve, the limit cycle becomes a homoclinic orbit after connecting with E_2^* and then it disappears. Next, we will investigate the dynamic properties and corresponding biological significance within the four regions and on the curves by analyzing the phase diagrams at the six locations (a)–(f) in Figure5 (b).

At location (a): $(-0.02, 0.0000000002)$ there exist trivial equilibrium E_0 (black dot in Figure 6(a)) and predator-free equilibria E_1 (red dot in Figure 6 (a)) and E_2 (blue dot in Figure 6(a)). But only the equilibrium E_2 is meaningful in the perspective of biology since the biomass of cyanobacteria must be greater than the aggregation amount according to the definition of model (1.3), and the parameter

of aggregation is $m = 30$ at this time. The predator-free equilibrium E_2 is a globally stable node here in the biological sense, which means that the population of fish will become extinct eventually and the cyanobacteria will remain at the corresponding density of E_2. The time series evolution and phase portrait of the model at location (a) can be seen as Figure 6(a).

The location (b): $(-0.02, 0)$, is on the SN curve. There exists a saddle-node equilibrium E^*_{sn} (blue dot in Figure 6(b)), which will evolve into two interior equilibria E^*_1 and E^*_2 as the two parameters enter region II from region I. In addition, the trivial equilibrium and the two predator-free equilibria also exist at this time. Similar to location (a), only E^*_{sn} and E_2 are meaningful from the biological point of view. Fish will eventually become extinct and the density of cyanobacteria will remain at the corresponding density of E_2 due to the instability of E^*_{sn}. The time series evolution and phase portrait near interior equilibrium E^*_{sn} are presented in Figure 6(b).

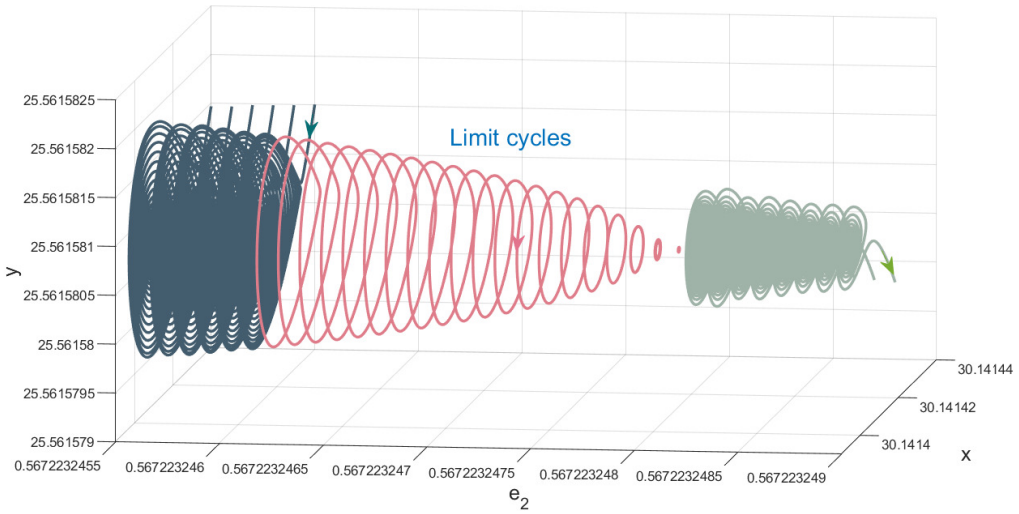

Figure 4. The progresses of homoclinic bifurcation and Hopf bifurcation in model (1.3) with the previous parameters and $e_1 = 3.174748196$.

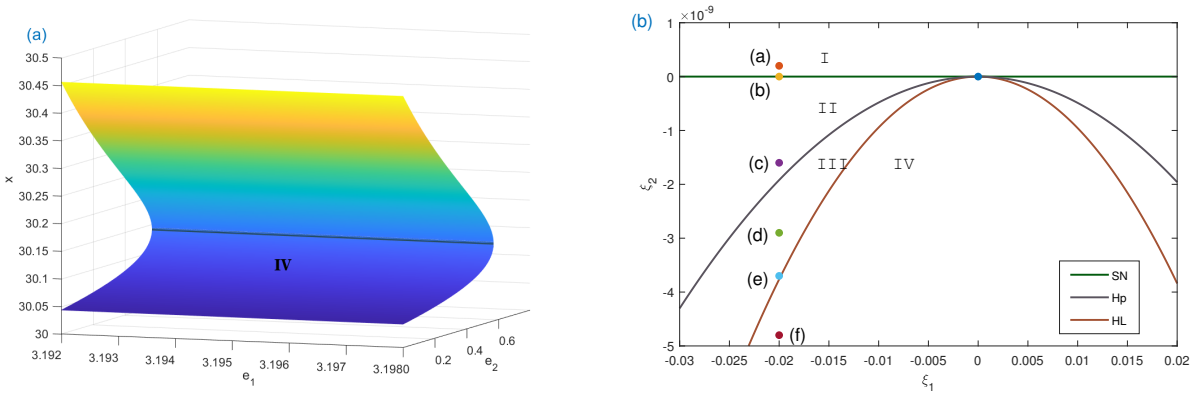

Figure 5. (a) The biomasses of prey at E^*_1 and E^*_2 with varying harvesting efforts. (b) Three bifurcation curves of model (1.3), which is another manifestation of lines between x^*_1 and x^*_2 in (a).

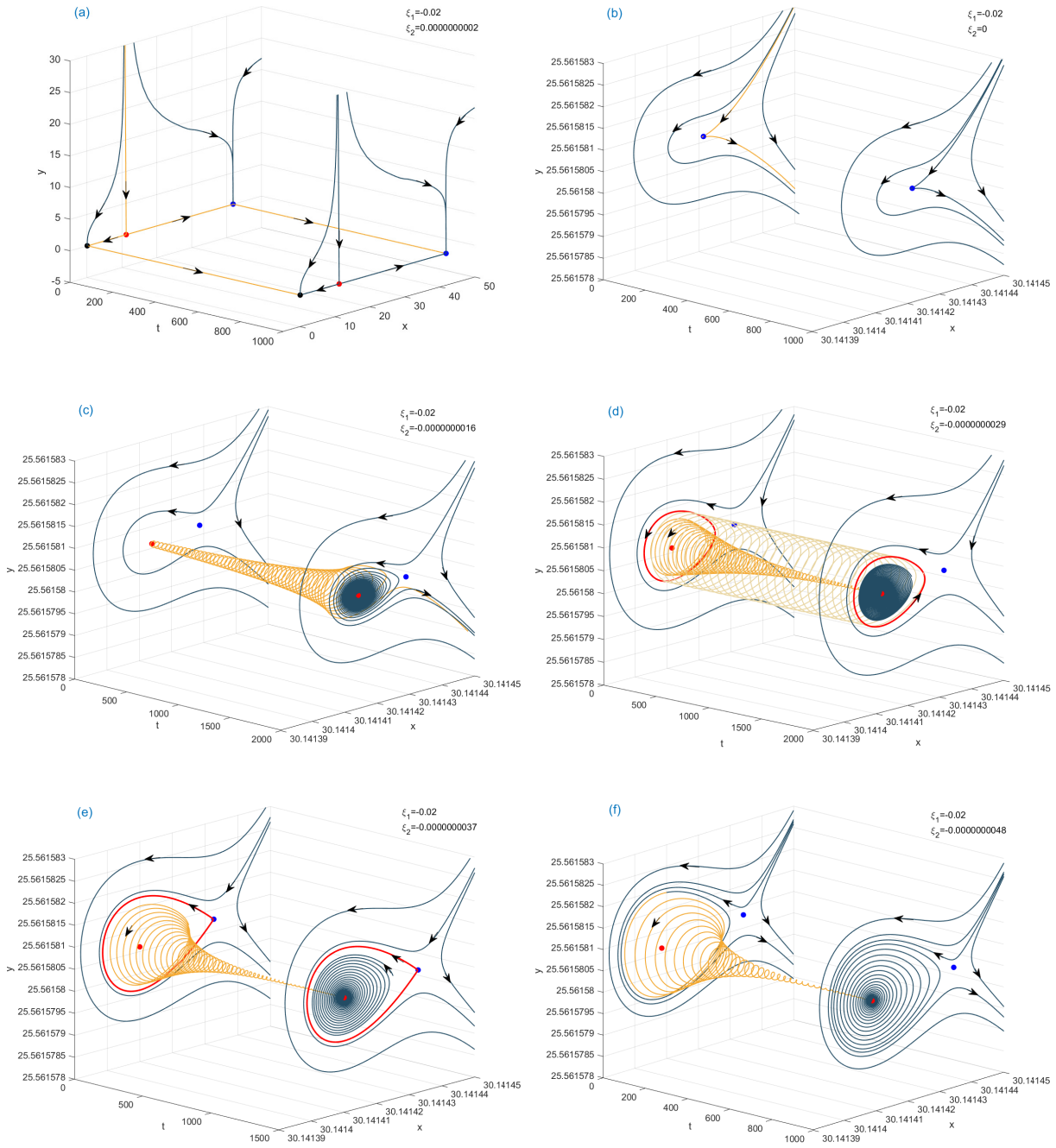

Figure 6. Phase portraits and time series evolution of model (1.3) with varying ξ_1 and ξ_2 around Bogdanov-Takens point $(0, 0)$.

There arise two interior equilibria E_1^* (red dot in Figure 6(c)) and E_2^* (blue dot in Figure 6(c)) from E_{sn}^* at location (c): $(-0.02, -0.0000000016)$; E_1^* and E_2^* are the unstable focus and unstable saddle respectively. The remaining equilibrium at this position has similar dynamic behavior as at position (b). Figure 6(c) presents the time series evolution and phase portrait around the interior equilibria. With the evolution of time, the final destiny of the two populations is consistent with that of position (b), that is, the fish is extinct and the population density of cyanobacteria tends to become stable.

The Hp curve has a significant influence on the dynamic behavior of model (1.3). When we move position (c) through the Hp curve to (d): $(-0.02, -0.0000000029)$, a Hopf bifurcation occurs in the model. A semistable limit cycle (red cycle in Figure 6(d)) arises around the interior equilibrium E_1^*; the value of the first Lyapunov number l_1 is -3149722.203π at this time, which indicates that the interior equilibrium E_1^* becomes stable after a supercritical Hopf bifurcation. With the evolution of time, the trajectory within a small range outside the limit cycle tends to the limit cycle, while the trajectory of the inside is far away from it and converges to the interior equilibrium E_1^*. Therefore, when the initial population densities of fish and cyanobacteria fall in different areas on the $\xi_1 - \xi_2$ plane, three different biological phenomena may occur. The first destiny is the same as the results for positions (a)–(c), which means that the fish will become extinct and the population density of cyanobacteria will remain at a stable state. The second result is that fish and cyanobacteria coexist and their population densities maintain periodic oscillation with time, but this periodic oscillation coexistence mode is unstable, and it leads to the third coexistence mode at stable focus E_1^* under the conditions a small disturbance from outside.

The limit cycle becomes larger gradually, and then connects with saddle equilibrium E_2^* to form a homoclinic orbit (red cycle in Figure 6(e)) in the process of moving down from position (d) to position (e): $(-0.02, -0.0000000037)$ on curve HL. The remaining equilibrium at this position has similar dynamic behavior as at position (d). The two species of fish and cyanobacteria will eventually coexist at the interior equilibrium E_1^* when the initial densities of the two populations falls within the homoclinic orbit. While on the homoclinic orbit or outside, the fish will eventually become extinct and the population density of cyanobacteria tends to the predator-free equilibrium of E_2 and then remains stable.

When the parameters are located at position (f): $(-0.02, -0.0000000048)$ in region IV, the homoclinic orbit disappears, and E_1^* is a stable focus and E_2^* is a saddle; the properties of other equilibria are consistent with those at position (e). The two populations will coexist at the interior equilibrium E_1^*, or the fish will become extinct and the cyanobacteria population will finally become stable depending on the initial population density. Therefore, an ideal ecological pattern can be guided to form by controlling the initial population density artificially.

6. Conclusions

This paper presented a cyanobacteria-fish model with two harvesting terms and a modified Holling type IV functional response function on the basis of a predator-prey model. The critical conditions were analyzed first to make certain the existence and stability of the potential equilibria in model (1.3), which is the preparatory work for the later theoretical analysis. We concluded that there is an economic equilibrium in model (1.3), and that the MSTY exists at the interior equilibrium E_1^* given certain parameters after analyzing the harvesting efforts. The numerical simulation suggests that a global

MSTY may not exist at equilibrium E_1^* for model (1.3), as illustrated in Figure 1. Nonetheless, the results presented in Figure 2 indicate that a local MSTY can be achieved for some given proportional coefficient of harvesting efforts λ. This has an enlightening effect on the managers of water ecological resources. That is, on the premise of ensuring that cyanobacteria do not break out and fish do not become extinct, they can choose to obtain the maximum and stable total yield at the MSTY point. Harvesting efforts e_1 and e_2 were chosen as our bifurcation parameters, and the existence of saddle-node bifurcation and Hopf bifurcation with codimension 1 and Bogdanov-Takens bifurcation with codimension 2 in the model are analyzed. The theoretical conditions of their occurrence have been concurrently given.

In the section of simulation analysis, the analysis of bifurcation theory for model (1.3) was further enriched with concrete numerical examples and corresponding biological explanations. The harvesting efforts of the two populations by humans affect the dynamic survival mode of the populations significantly. The harvesting efforts were selected for different regions in Figure 5(b), and the corresponding phase portraits and time series evolution of model (1.3) can be seen in Figure 6(a)–(f). Initially, the fish population goes extinct, then the two populations coexist in periodic oscillations within a certain range, and finally, they coexist at the internal equilibrium. According to the phase portraits and time series evolution of the model when the parameters are taken in different regions on the bifurcation diagram, we obtained the dynamic behaviors and explained the corresponding biological significances. This provides inspiration for the water ecological resource managers to formulate reasonable harvesting strategies. That is, they can promote the development of the two populations to reach their expected target by controlling the initial population densities of cyanobacteria and fish and adopting harvesting efforts with corresponding intensity. It is also one of the important contributions of our paper. In addition, formulating mature and practical harvesting strategies in further research is necessary.

Based on the results of our research, it is worth noting that appropriate physical harvesting can induce significant changes in the coexistence mode of cyanobacteria and fish through the utilization of the dynamic transition between saddle-node bifurcation and Hopf bifurcation. In addition, Hopf bifurcation can result in a periodic oscillation coexistence mode between cyanobacteria and fish. Although the periods of these oscillations along different closed trajectories may differ, the average number of cyanobacteria and fish should remain constant within one cycle. Therefore, this research shows that cyanobacteria and fish can gradually form a new cyclic coexistence mode through physical harvesting strategies and biological algae control technologies. Furthermore, the numerical simulation results of Bogdanov-Takens bifurcation suggest that small changes in ecological environmental factors could lead to different coexistence modes of cyanobacteria and fish. Thus, when implementing physical harvesting strategies and ecological algae control technologies in the field, it is necessary to effectively and timely control the implementation process and related quantity limits based on the actual situation in the field.

Although this study has yielded some good results, its research results were mainly obtained through the evolutionary characteristics of bifurcation dynamics, which had certain limitations. At the same time, the construction of the model (1.2) overlooked some of the interaction mechanisms between cyanobacteria and fish, which could lead to incomplete analysis of their interaction mechanisms. The influence of different harvesting terms on the dynamic behaviors of the model needs further consideration, and we will verify the reliability of the model through experiments in follow-up work. Of course, in order to make our model reflect the real situation within a small range of error, we need to

improve the model according to many factors. For example, after introducing other species, a multi-prey or multi-predator model can be constructed according to a series of survival relationships between them. We can further enhance our model by incorporating the spatial diffusion behavior of the species. This can help us better understand the nature of the relationship between fish and cyanobacteria by considering the different population distributions.

Acknowledgments

This work was supported by the National Natural Science Foundation of China (Grant No. 61871293 and No. 61901303), and the National Key Research and Development Program of China (Grant No. 2018YFE0103700).

Conflict of interest

All authors declare that there is no conflict of interest.

References

1. H. W. Paerl, T. G. Otten, Harmful cyanobacterial blooms: Causes, consequences, and controls, *Microb. Ecol.*, **65** (2013), 995–1010. https://doi.org/10.1007/s00248-012-0159-y
2. A. Serrà, L. Philippe, F. Perreault, S. Garcia-Segura, Photocatalytic treatment of natural waters. reality or hype? the case of cyanotoxins remediation, *Water Res.*, **188** (2021), 116543. https://doi.org/10.1016/j.watres.2020.116543
3. A. Włodarczyk, T. T. Selão, B. Norling, P. J. Nixon, Newly discovered Synechococcus sp. PCC 11901 is a robust cyanobacterial strain for high biomass production, *Commun. Biol.*, **3** (2020), 215. https://doi.org/10.1038/s42003-020-0910-8
4. A. Shahid, M. Usman, Z. Atta, S. G. Musharraf, S. Malik, A. Elkamel, et al., Impact of wastewater cultivation on pollutant removal, biomass production, metabolite biosynthesis, and carbon dioxide fixation of newly isolated cyanobacteria in a multiproduct biorefinery paradigm, *Bioresour. Technol.*, **333** (2021), 125194. https://doi.org/10.1016/j.biortech.2021.125194
5. K. Chandrasekhar, T. Raj, S. V. Ramanaiah, G. Kumar, J. R. Banu, S. Varjani, et al., Algae biorefinery: A promising approach to promote microalgae industry and waste utilization, *J. Biotechnol.*, **345** (2022), 1–16. https://doi.org/10.1016/j.jbiotec.2021.12.008
6. B. Öğlü, U. Bhele, A. Järvalt, L. Tuvikene, H. Timm, S. Seller, et al., Is fish biomass controlled by abiotic or biotic factors? results of long-term monitoring in a large eutrophic lake, *J. Great Lakes Res.*, **46** (2020), 881–890. https://doi.org/10.1016/j.jglr.2019.08.004
7. R. J. Shen, X. H. Gu, H. H. Chen, Z. G. Mao, Q. F. Zeng, E. Jeppesen, Combining bivalve (Corbicula fluminea) and filter-feeding fish (Aristichthys nobilis) enhances the bioremediation effect of algae: An outdoor mesocosm study, *Sci. Total Environ.*, **727** (2020), 138692. https://doi.org/10.1016/j.scitotenv.2020.138692

8. C. Arancibia-Ibarra, P. Aguirre, J. Flores, P. V. Heijster, Bifurcation analysis of a predator-prey model with predator intraspecific interactions and ratio-dependent functional response, *Appl. Math. Comput.*, **402** (2021), 126152. https://doi.org/10.1016/j.amc.2021.126152
9. X. L. Zou, Q. W. Li, J. L. Lv, Stochastic bifurcations, a necessary and sufficient condition for a stochastic Beddington-DeAngelis predator-prey model, *Appl. Math. Lett.*, **117** (2021), 107069. https://doi.org/10.1016/j.aml.2021.107069
10. F. Souna, A. Lakmeche, S. Djilali, Spatiotemporal patterns in a diffusive predator-prey model with protection zone and predator harvesting, *Chaos Solitons Fractals*, **140** (2020), 110180. https://doi.org/10.1016/j.chaos.2020.110180
11. T. T. Liu, L. J. Chen, F. D. Chen, Z. Li, Dynamics of a Leslie–Gower model with weak Allee effect on prey and fear effect on predator, *Int. J. Bifurcat. Chaos*, **33** (2023), 2350008. https://doi.org/10.1142/S0218127423500086
12. X. B. Zhang, H. Y. Zhao, Bifurcation and optimal harvesting of a diffusive predator-prey system with delays and interval biological parameters, *J. Theor. Biol.*, **363** (2014), 390–403. https://doi.org/10.1016/j.jtbi.2014.08.031
13. T. K. Ang, H. M. Safuan, Dynamical behaviors and optimal harvesting of an intraguild prey-predator fishery model with Michaelis-Menten type predator harvesting, *Biosystems*, **202** (2021), 104357. https://doi.org/10.1016/j.biosystems.2021.104357
14. M. El-Shahed, A. M. Al-Dububan, Deterministic and stochastic fractional-order Hastings-Powell food chain model, *CMC*, **70** (2022), 2277–2296. https://doi.org/10.32604/cmc.2022.019314
15. M. G. Mortuja, M. K. Chaube, S. Kumar, Dynamic analysis of a predator-prey system with non-linear prey harvesting and square root functional response, *Chaos Solitons Fractals*, **148** (2021), 111071. https://doi.org/10.1016/j.chaos.2021.111071
16. E. Bellier, B. E. Sæther, S. Engen, Sustainable strategies for harvesting predators and prey in a fluctuating environment, *Ecol. Model.*, **440** (2021), 109350. https://doi.org/10.1016/j.ecolmodel.2020.109350
17. A. Mezouaghi, S. Djilali, S. Bentout, K. Biroud, Bifurcation analysis of a diffusive predator-prey model with prey social behavior and predator harvesting, *Math. Method Appl. Sci.*, **45** (2022), 718–731. https://doi.org/10.1002/mma.7807
18. J. Al-Omari, G. Gumah, S. Al-Omari, Dynamics of a harvested stage-structured predator-prey model with distributed maturation delay, *Math. Method Appl. Sci.*, **45** (2022), 761–769. https://doi.org/10.1002/mma.7810
19. B. F. Xie, Z. C. Zhang, N. Zhang, Influence of the fear effect on a Holling type II prey-predator system with a Michaelis-Menten type harvesting, *Int. J. Bifurcat. Chaos*, **31** (2021), 2150216. https://doi.org/10.1142/S0218127421502163
20. D. Y. Wu, H. Y. Zhao, Y. Yuan, Complex dynamics of a diffusive predator-prey model with strong Allee effect and threshold harvesting, *J. Math. Anal. Appl.*, **469** (2019), 982–1014. https://doi.org/10.1016/j.jmaa.2018.09.047

21. S. Li, S. L. Yuan, Z. Jin, H. Wang, Bifurcation analysis in a diffusive predator-prey model with spatial memory of prey, Allee effect and maturation delay of predator, *Int. J. Differ. Equation*, **357** (2023), 32–63. https://doi.org/10.1016/j.jde.2023.02.009

22. Y. Y. Lv, L. J. Chen, F. D. Chen, Z. Li, Stability and bifurcation in an SI epidemic model with additive Allee effect and time delay, *Int. J. Bifurcat. Chaos*, **31** (2021), 2150060. https://doi.org/10.1142/S0218127421500607

23. D. Y. Wu, H. Y. Zhao, Spatiotemporal dynamics of a diffusive predator-prey system with Allee effect and threshold hunting, *Int. J. Nonlinear. Sci*, **30** (2020), 1015–1054. https://doi.org/10.1007/s00332-019-09600-0

24. W. X. Wang, Y. B. Zhang, C. Z. Liu, Analysis of a discrete-time predator-prey system with Allee effect, *Ecol. Complex.*, **8** (2011), 81–85. https://doi.org/10.1016/j.ecocom.2010.04.005

25. D. Sen, S. Ghorai, M. Banerjee, Allee effect in prey versus hunting cooperation on predator-enhancement of stable coexistence, *Int. J. Bifurcat. Chaos*, **29** (2019), 1950081. https://doi.org/10.1142/S0218127419500810

26. H. Molla, S. Sarwardi, S. R. Smith, M. Haque, Dynamics of adding variable prey refuge and an Allee effect to a predator-prey model, *Alex. Eng. J.*, **61** (2022), 4175–4188. https://doi.org/10.1016/j.aej.2021.09.039

27. D. Barman, J. Roy, H. Alrabaiah, P. Panja, S. P. Mondal, S. Alam, Impact of predator incited fear and prey refuge in a fractional order prey predator model, *Chaos Solitons Fractals*, **142** (2021), 110420. https://doi.org/10.1016/j.chaos.2020.110420

28. W. Q. Yin, Z. Li, F. D. Chen, M. X. He, Modeling Allee effect in the Leslie-Gower predator-prey system incorporating a prey refuge, *Int. J. Bifurcat. Chaos*, **32** (2022), 2250086. https://doi.org/10.1142/S0218127422500869

29. S. Y. Huang, H. G. Yu, C. J. Dai, Z. L. Ma, Q. Wang, M. Zhao, Dynamic analysis of a modified algae and fish model with aggregation and Allee effect, *Math. Biosci. Eng.*, **19** (2022), 3673–3700. https://doi.org/10.3934/mbe.2022169

30. G. Bapan, T. Kar, T. Legovic, Sustainability of exploited ecologically interdependent species., *Popul. Ecol.*, **56** (2014), 527–537. https://doi.org/10.1007/s10144-014-0436-3

31. P. Paul, T. K. Kar, Impacts of invasive species on the sustainable use of native exploited species, *Ecol. Model.*, **340** (2016), 106–115. https://doi.org/10.1016/j.ecolmodel.2016.09.002

32. X. X. Liu, Q. D. Huang, Analysis of optimal harvesting of a predator-prey model with Holling type IV functional response, *Ecol. Complex.*, **42** (2020), 100816. https://doi.org/10.1016/j.ecocom.2020.100816

33. Z. C. Shang, Y. H. Qiao, L. J. Duan, J. Miao, Bifurcation analysis in a predator-prey system with an increasing functional response and constant-yield prey harvesting, *Math. Comput. Simulat.*, **190** (2021), 976–1002. https://doi.org/10.1016/j.matcom.2021.06.024

34. D. P. Hu, H. J. Cao, Stability and bifurcation analysis in a predator-prey system with Michaelis-Menten type predator harvesting, *Nonlinear Anal. Real World Appl.*, **33** (2017), 58–82. https://doi.org/10.1016/j.nonrwa.2016.05.010

35. J. C. Huang, S. G. Ruan, J. Song, Bifurcations in a predator-prey system of Leslie type with generalized Holling type III functional response, *J. Differ. Equations*, **257** (2014), 1721–1752. https://doi.org/10.1016/j.jde.2014.04.024

Appendix A

$$\alpha_{10} = \alpha_{02} = \alpha_{12} = \alpha_{03} = \beta_{01} = \beta_{02} = \beta_{12} = \beta_{03} = 0,$$

$$\alpha_{01} = -\frac{x_1^* - m}{\left(x_1^* - m\right)^2 + b\left(x_1^* - m\right) + a}, \quad \alpha_{11} = \frac{\left(x_1^* - m\right)^2 - a}{\left[\left(x_1^* - m\right)^2 + b\left(x_1^* - m\right) + a\right]^2},$$

$$\alpha_{20} = \frac{r}{kn}\left(n + k - 3x_1^*\right) + \frac{y_1^*\left[-\left(x_1^* - m\right)^3 + 3a\left(x_1^* - m\right) + ab\right]}{\left[\left(x_1^* - m\right)^2 + b\left(x_1^* - m\right) + a\right]^3},$$

$$\alpha_{30} = -\frac{3r}{kn} - \frac{y_1^*\left[7\left(x_1^* - m\right)^2 + 5b\left(x_1^* - m\right) + b^2 - a\right]}{\left[\left(x_1^* - m\right)^2 + b\left(x_1^* - m\right) + a\right]^3} + \frac{y_1^*\left[2\left(x_1^* - m\right) + b\right]^3}{\left[\left(x_1^* - m\right)^2 + b\left(x_1^* - m\right) + a\right]^4},$$

$$\alpha_{21} = \frac{-\left(x_1^* - m\right)^3 + 3a\left(x_1^* - m\right) + ab}{\left[\left(x_1^* - m\right)^2 + b\left(x_1^* - m\right) + a\right]^3}, \quad \beta_{10} = -\frac{\beta y_1^*\left[\left(x_1^* - m\right)^2 - a\right]}{\left[\left(x_1^* - m\right)^2 + b\left(x_1^* - m\right) + a\right]^2},$$

$$\beta_{11} = -\frac{\beta\left[\left(x_1^* - m\right)^2 - a\right]}{\left[\left(x_1^* - m\right)^2 + b\left(x_1^* - m\right) + a\right]^2}, \quad \beta_{20} = \frac{\beta y_1^*\left[\left(x_1^* - m\right)^3 - 3a\left(x_1^* - m\right) - ab\right]}{\left[\left(x_1^* - m\right)^2 + b\left(x_1^* - m\right) + a\right]^3},$$

$$\beta_{30} = \frac{\beta y_1^*\left[7\left(x_1^* - m\right)^2 + 5b\left(x_1^* - m\right) + b^2 - a\right]}{\left[\left(x_1^* - m\right)^2 + b\left(x_1^* - m\right) + a\right]^3} - \frac{\beta y_1^*\left[2\left(x_1^* - m\right) + b\right]^3}{\left[\left(x_1^* - m\right)^2 + b\left(x_1^* - m\right) + a\right]^4},$$

$$\beta_{21} = \frac{\beta\left[\left(x_1^* - m\right)^3 - 3a\left(x_1^* - m\right) - ab\right]}{\left[\left(x_1^* - m\right)^2 + b\left(x_1^* - m\right) + a\right]^3}.$$

Appendix B

$$c_{00}(\xi_1,\xi_2) = \alpha_{01}(\xi_1,\xi_2)\, q_{00}(\xi_1,\xi_2) - p_{00}(\xi_1,\xi_2)\, q_{01}(\xi_1,\xi_2),$$

$$c_{10}(\xi_1,\xi_2) = \alpha_{01}(\xi_1,\xi_2)\beta_{10}(\xi_1,\xi_2) + \alpha_{11}(\xi_1,\xi_2)\, q_{00}(\xi_1,\xi_2) - p_{00}(\xi_1,\xi_2)\beta_{11}(\xi_1,\xi_2) - p_{10}(\xi_1,\xi_2)\, q_{01}(\xi_1,\xi_2),$$

$$c_{01}(\xi_1,\xi_2) = p_{10}(\xi_1,\xi_2) + q_{01}(\xi_1,\xi_2) - \frac{\alpha_{11}(\xi_1,\xi_2)\, p_{00}(\xi_1,\xi_2)}{\alpha_{01}(\xi_1,\xi_2)}, \quad c_{02}(\xi_1,\xi_2) = \frac{\alpha_{11}(\xi_1,\xi_2)}{\alpha_{01}(\xi_1,\xi_2)},$$

$$c_{20}(\xi_1,\xi_2) = \alpha_{01}\beta_{20}(\xi_1,\xi_2) + \alpha_{11}\beta_{10}(\xi_1,\xi_2) - \alpha_{20}(\xi_1,\xi_2)\, q_{01}(\xi_1,\xi_2) - p_{10}(\xi_1,\xi_2)\beta_{11}(\xi_1,\xi_2),$$

$$c_{11}(\xi_1,\xi_2) = \beta_{11}(\xi_1,\xi_2) + 2\alpha_{20}(\xi_1,\xi_2) - \frac{\alpha_{11}(\xi_1,\xi_2)\, p_{10}(\xi_1,\xi_2)}{\alpha_{01}(\xi_1,\xi_2)} + \frac{\alpha_{11}^2(\xi_1,\xi_2)\, p_{00}(\xi_1,\xi_2)}{\alpha_{01}^2(\xi_1,\xi_2)}.$$

AIMS Press